Supplementary information

The reorganization energy of intermolecular hole hopping between dyes anchored to surfaces

Davide Moia,,[a] Valérie Vaissier,[a] Ismael López-Duarte,[b] Tomás Torres,[b,c] Mohammad K. Nazeeruddin,[d] Brian C. O'Regan,[e] Jenny Nelson,[a] Piers R. F. Barnes[a,]***

[a]Department of Physics, Imperial College London, SW7 2AZ, UK

[b]Departamento de Química Orgánica, Facultad de Ciencias, Universidad Autónoma de Madrid, E-28049 Madrid, Spain

[c]IMDEA-Nanociencia, c/Faraday, 9, Campus de Cantoblanco, E-28049 Madrid, Spain

[d]Laboratory of Photonics and Interfaces, Department of Chemistry and Chemical Engineering, Swiss Federal Institute of Technology, Station 6, CH-1015 Lausanne, Switzerland.

[e]Department of Chemistry, Imperial College London, SW7 2AZ, UK

* davide.moia11@imperial.ac.uk

** piers.barnes@imperial.ac.uk

1. Experimental details

1.1 Film preparation and concentration measurement

Conductive FTO glass slides (TEC-15) were used as substrates for the samples. The slides were cleaned with soap, rinsed with deionized water, acetone and isopropanol. They finally underwent a heating process at 450°C for 30 minutes. TiO_2 paste (Dyesol 18 NR-T) was deposited on the FTO glass via doctor blading. The films were sintered at 450°C for 30 minutes (10 minutes for the heating ramp), the resulting film thicknesses were ~ 7µm measured using a profilometer.

Samples were stored at room temperature and used within one day after sintering. Before the dyeing step, the films were left at 120°C for about 15 minutes. The dyeing process was performed at room temperature in the conditions described in Table S1. The last column represents the dyes volume concentration on the TiO_2 film after dyeing (dye loading).

Table S1. Dyeing conditions for the materials investigated in this work. Solvents acronyms correspond to: acetonitrile (ACN), tert-butyl alcohol (TBA), dichloromethane (DCM), ethanol (EtOH) and dimethyl sulfoxide (DMSO).

Dye	**Solvent**	**Concentration** [mM]	**Dyeing time** [hrs]	c_0 [10^{19} cm^{-3}]
Z907	ACN:TBA 1:1	0.3	20	9.1 ± 1.4
N820	ACN:TBA 1:1	0.3	20	9.6 ± 1.5
N719	ACN:TBA 1:1	0.3	20	6.6 ± 1.2
D131	ACN:TBA 1:1	0.1	3.5	8.8 ± 1.4
D149	ACN:TBA 1:1	0.06	3.5	6.6 ± 1.0
ZnPP	DMSO	0.3	20	4.2 ± 0.7
TT-1	EtOH	0.1	20	13 ± 2
TT-35	DCM	0.1	20	4.4 ± 0.7
A2	DCM	0.1	20	7.0 ± 1.1
A5	DCM	0.1	20	2.7 ± 0.4

The volume concentration of dye molecules (c_0) attached to the TiO_2 mesoporous films upon sensitization was determined via UV-vis spectroscopy. UV-vis measurement performed on the film after sensitization gives direct information on the dye loading, but in some cases it suffers from variation of the species light absorption spectrum due to their adsorption on the TiO_2 surface.[1] In this case, dye desorption experiments can be used to measure the amount of molecules sensitizing the known volume of the mesoporous TiO_2 film.[2]

Alternatively, one can measure the UV-vis spectrum of the known amount of solution used to sensitize the film before and after the dyeing process. The dye solution depletion is then correlated to the amount of dye molecules that have been adsorbed on the surface of the nanocrystalline TiO_2 film. This method is potentially more robust with respect to the changes that may occur to the molecules during desorption experiments (Figure S1). On the other hand, it does not account for the dyes weakly adsorbed that are removed during the rinsing of the sample.

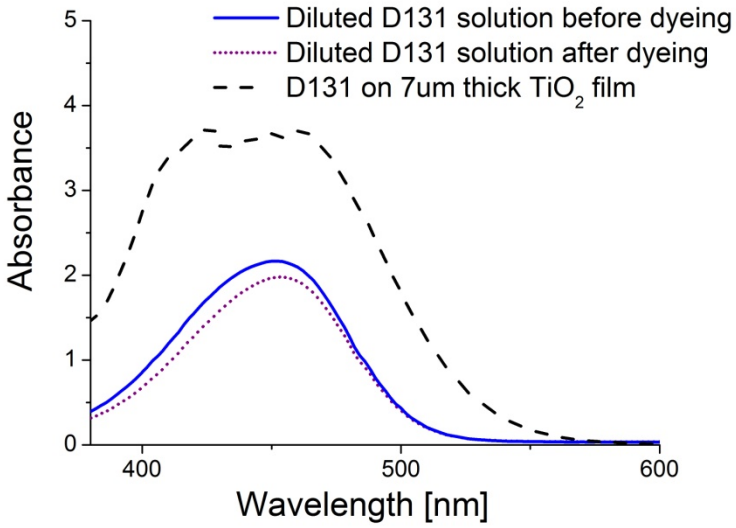

Figure S1. D131 dyeing of TiO_2 films. The spectrum of the dyed film shows very high absorbance at the peak (transmittance is below the resolution of the detector). Also, the shape of the absorbance is broadened if compared with the dye in solution due to adsorption on the TiO_2 surface and interaction between dyes. The measurement of the solution absorbance before and after the dyeing process is a possible way to estimate the dye loading c_0.

1.2 Dye reversibility and dye desorption

Repeated cyclic voltammetry (CV) measurements on the same sample showed a decrease in the positive current peak for all the systems we considered (see next section for current peak evaluation). Interestingly, the extent of this decrease is negatively correlated to the reversibility of the dye molecule (Figure S2 left). N719 in particular showed very poor reversibility, consistent with the very short lifetime of the oxidized molecule.[3] For most dyes, and particularly in the case of the indoline dyes, repeated CV measurements led to partial desorption of dyes from the film surface.

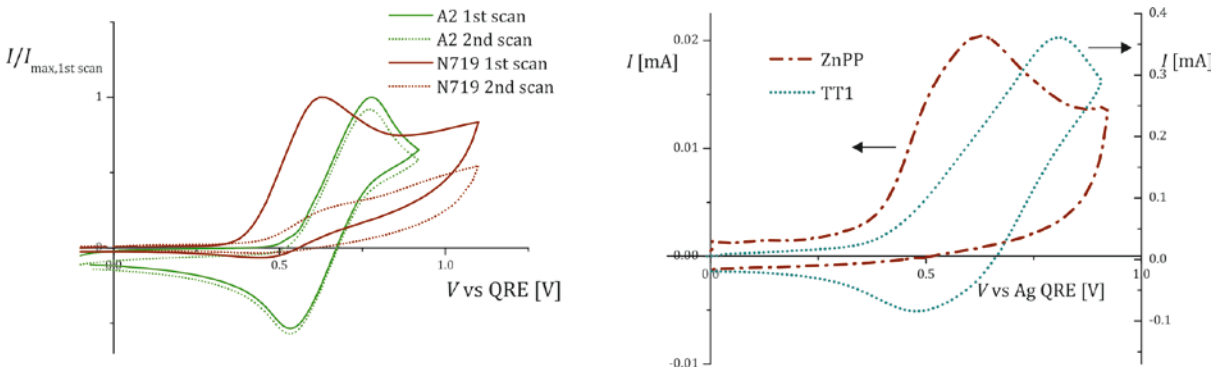

Figure S2. (left) Cyclic voltammograms of A2 (scan rate 0.3 V/s) and N719 (scan rate 0.5 V/s) attached to TiO_2 nanocrystalline films showing the first cycle (solid lines) and the second cycle (dashed lines). The magnitude of the positive redox peak in the second scan correlates with the negative peak of the first scan. (Right) cyclic voltammograms of ZnPP and TT-1 dye sensitized TiO_2 performed at a scan rate of 0.1 V/s. The former dye shows poor reversibility, whereas the second exhibits a double component response in the electrochemical response.

To minimize these problems of reversibility a fresh sample was therefore used for each measurement of the apparent diffusion coefficient in our temperature dependent CV study. Analysis was performed only on the initial current peak resulting from the forward voltage sweep.

The electrochemical induced degradation of dyes anchored on the FTO surface has been suggested as a possible reason for the decrease in the current density peak over consecutive CV measurements. The limited reversibility has therefore been ascribed to the holes being unable to access the population of dyes adsorbed on the TiO_2 through the dyes adsorbed on the FTO.[4,3] In the same study, desorption was instead excluded as the main factor causing the degradation of the CV curves, since only limited variation of the UV-vis spectrum of the film after multiple cycling was observed which did not correspond to the much more substantial drop in electrochemical response. Figure S3 shows the temperature dependence of the peak oxidation current of films of N719 dye, with the inset clearly showing the irreversible nature of the process. Since the kinetics of degradation is, in this case, comparable to the hopping of holes beyond the layer of molecules at the FTO substrate, it is not meaningful to interpret these data in terms of an activation energy for hole transport. Similar irreversible behaviour was recorded for the dye ZnPP, as shown in the right plot of Figure S2. In the same graph, we also report the shape of a cyclic voltammogram performed on a TT-1 dye sensitized film. In our study, we assumed that the current density peak for this material still represents an indication of the ability of holes to diffuse in the monolayer, despite the presence of two oxidations in the electrochemical response.

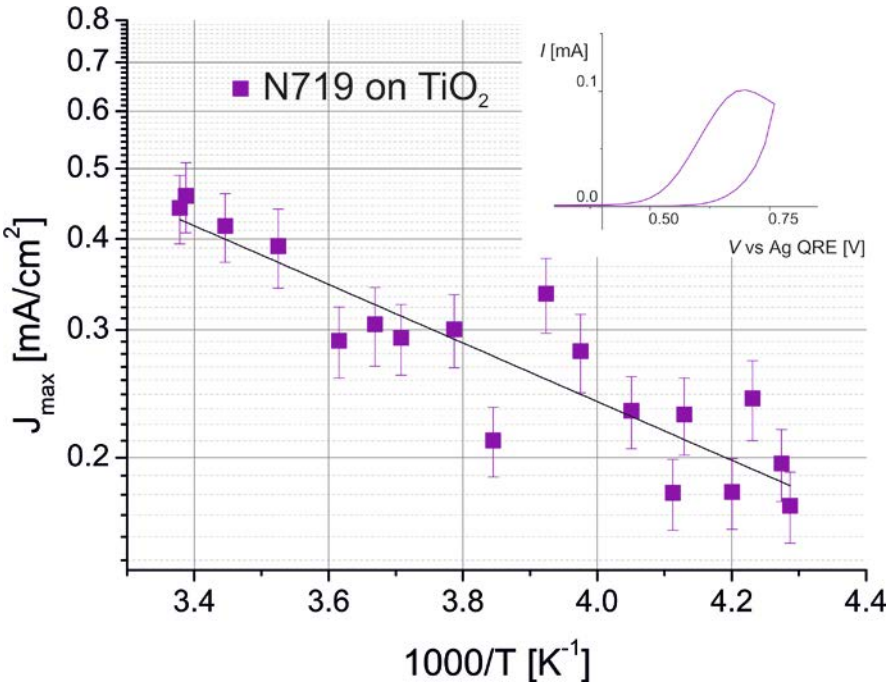

Figure S3. Arrhenius plot of current density peaks of temperature dependent CV performed on N719 dye sensitized TiO_2 films with 0.3 V/s scan rate. The electrochemical response of the samples showed almost no reversibility (see inset). The extracted activation energy is 79.4 meV.

1.3 Quasi reference electrode

The use of a silver wire as quasi reference electrode of the electrochemical cell does not constrain the temperature range spanned during the experiment. The wire was placed at about 1 mm distance from the dyed film to minimize the contribution of the solvent series resistance. The potential of the silver wire is typically close to the potential of Ag/AgCl reference electrode (0.209 vs NHE for the case of 3M NaCl electrodes).[5] In some cases, when comparing CV curves performed in the same experiment, variations of up to 300 mV of the chemical potential of the silver wire could be observed over tens of measurements. Here, we assume that these changes occurred slowly relative to the scan rate adopted during our measurements and we neglect their effect on the effective potential scan rate applied to the system.

1.4 CV curve: baseline subtraction

To extract the apparent hole hopping diffusion coefficient from a cyclic voltamogram, the different contributions to the observed current should be accounted for. The possible contributions to the current at the working electrode are:

Holes injected from the FTO substrate into the dyed film on the TiO_2 nanoparticulate surface and hopping across the dye monolayer: this is the useful component to the observed current that can be used to calculate the apparent diffusion coefficient.

Holes injected from the FTO substrate into dyes anchored to the FTO surface outside the region of the TiO_2 film: the oxidation/reduction of these additional molecules gives rise to an additional spurious current component whose redox peaks almost overlap those of the hole hopping component. Neglecting this contribution can lead to an overestimation of D_{app}. For this reason, we ensured that the electrolyte wet as small a fraction of the bare dyed FTO as possible to minimize current unrelated to hole transport across the dyed TiO_2 surface. This was particularly important when working with relatively small active areas which were required to reduce the effects of series resistance on effective scan rate (see section 2.2). Note that the peak current density of this component increases linearly with the scan rate, whereas the hole hopping current density signal increases with the square root of the scan rate (see equation S2.3 in the next chapter). The use of low enough scan rates results in the electrochemical signal of dyes anchored to the bare FTO surface to be negligible.

Current due to substrate capacitance: this component results from charging the effective capacitance of the FTO substrate and the TiO_2 film to the voltage set by the potentiostat. In the case of a constant capacitance value C whose voltage is linearly changed with a scan rate v, this current would reach and saturate at the value $I = Cv$ with a time constant $\tau = RC$, where R is the series resistance of the circuit.[6] This constant baseline can then be easily subtracted from the overall current profile. The actual current that we observed in the case of a bare FTO and a bare TiO_2 film does not show a saturation value, meaning that the differential capacitance of the substrate is not constant with voltage (see examples shown in Figure S4). These curves suggest that oxidation of impurities may also be taking place (the current remains positive during the reverse scan for the measurement on TiO_2). This contribution is typically very low in our system compared to the peak current density due to the redox of the dyes.

Faradaic current from the working electrode to the solution: this spurious component was observed occasionally in some of our measurements where, due to the presence of a meniscus, the electrolyte was in contact with the working electrode connection (a thin copper sheet used to contact the FTO glass to the potentiostat lead). This resulted in a baseline current component which showed a linear dependence on the voltage applied between the WE and the RE (see Figure S4). It was found to be independent of the scan rate. We assume its presence does not affect the redox current related to the hole hopping between dyes on TiO_2. Its effects were corrected for by subtracting a linear baseline from the observed current measurements.

The peak current, I_p, used to estimate the apparent diffusion coefficient of hole hopping, was determined after subtracting a baseline from the measured current. This was estimated by fitting a straight line to the linear section of the CV curve before the onset of the oxidation peak (see Figure S5). This approach removes the contribution of the Faradaic component (as described above), if any, and limits the effect of the substrate behavior.

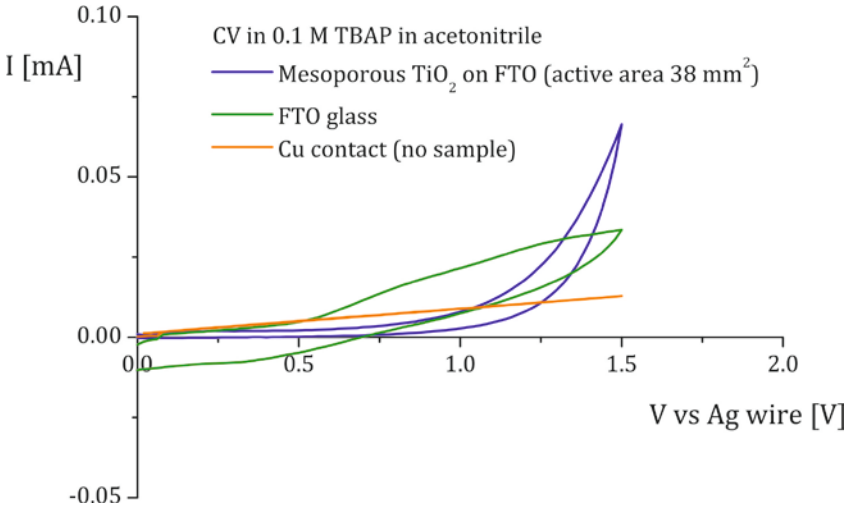

Figure S4. CV measurements performed at a scan rate of 0.3 V/s in 0.1M TBAP in acetonitrile showing some of the baseline involved in our experiments. The current components related to the FTO and the mesoporous TiO_2 electrolyte interface are shown. The linear profile corresponds to the current flowing in the electrochemical cell in the case where no sample is measured and the wet contact exchanges charges

with the electrolyte giving rise to a faradaic behavior (no change in the magnitude of the current is observed when the scan rate is changed).

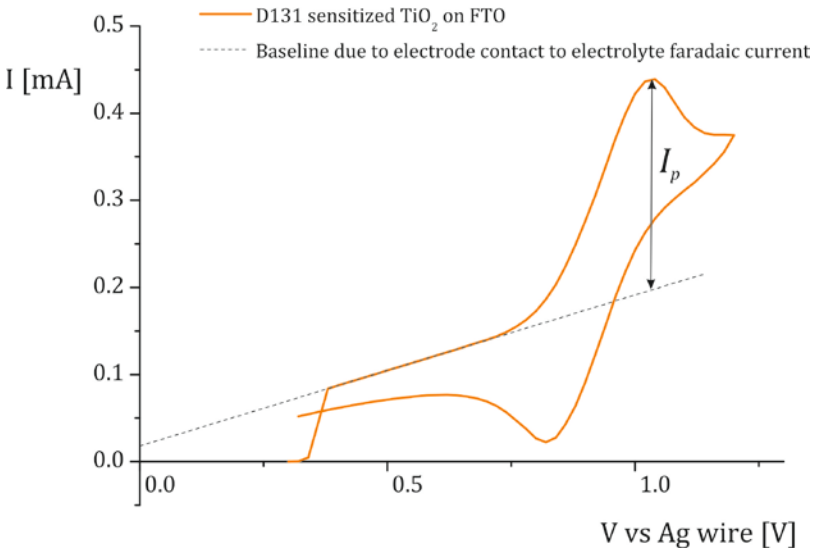

Figure S5. CV measurement on D131 sensitized TiO_2 films on FTO performed at a scan rate of 0.3 V/s in 0.1M TBAP in acetonitrile. The background current (highlighted by the fitting dashed line) is very evident in this measurement and it is mainly due to the contact between the electrolyte and the working electrode. The extraction of I_p in this case was done on the overall current after the subtraction of this linear profile.

1.5 Temperature dependent measurement

Acetonitrile, the solvent used in this study, is a relatively volatile solvent (boiling point is about 82°C), therefore temperature values higher than room temperature were avoided to prevent significant evaporation from the electrolyte solution which would have led to uncertainty on its concentration. However, considering typical expected activation energy values (between 200 and 300 meV), a relatively big variation in temperature was needed in order to detect evident variations in the apparent diffusion coefficient and to extract a trend with acceptable accuracy. A cuvette was used as electrochemical cell and its temperature was controlled by means of a bath of acetone in which dry ice was added in order to cool down the cell, down to a minimum temperature of about 230K (the freezing point of Acetonitrile is 228K). The temperature was monitored by means of a thermocouple inserted in the cell through a sealed glass capillary which was dipped in the electrolyte solution. From calibration measurements using a low temperature thermometer or a second thermocouple

directly inserted in the solution, we expect accuracy in the temperature determination within 1K.

We note that variations in temperature lead to changes in the dielectric constant of the environment (typically solvents show higher dielectric constant values at lower temperature). This implies that the surrounding dielectric medium is different at different temperature and the resulting reorganization energy related to the charge transfer process is in fact a function of temperature. However, in our case, acetonitrile is a relatively polar solvent. Given the dependence of the outer sphere component of the reorganization energy[7] on the solvent polarity, we neglect this factor in our analysis.

2. Data analysis

2.1 1D diffusion model: the semi-infinite slab approximation

Extracting the holes apparent diffusion coefficient from the system described in the main text of this work and in this document can be treated as a one dimensional diffusion problem described by the following equations:

$$\begin{cases} \dfrac{\partial c_h(x,t)}{\partial t} = D_{app}\dfrac{\partial^2 c_h(x,t)}{\partial x^2} \\ c_h(0,t) = \dfrac{c_0}{1+e^{\frac{q(E_0-E(t))}{k_BT}}} \\ E(t) = E(t=0) + \nu \cdot t \\ \dfrac{\partial c_h(d,t)}{\partial x} = 0 \\ c_h(x,0) = \dfrac{c_0}{1+e^{\frac{q(E_0-E(t=0))}{k_BT}}} \end{cases} \qquad \text{Eq. S2.1}$$

In this model, $c_h(x,t)$ is the volume concentration of holes [cm^{-3}] function of the position x (ranging from 0, the position of the FTO/TiO_2 interface, to d, the total thickness of the film)

and the time t. D_{app} is the holes apparent diffusion coefficient [cm^2/s], c_0 is the concentration of redox sites [cm^{-3}], q is the elementary charge [C], $E(t)$ is the chemical potential [V] applied to the working electrode function of time, E_0 is the formal oxidation potential of the dye [V], k_B is the Boltzmann constant [$J\ K^{-1}$], T is temperature [K], and v is the applied scan rate [$V\ s^{-1}$]. The first boundary condition is represented by Nernst equation, which defines the concentration of holes at the FTO / dyed TiO_2 interface ($x = 0$). Here, we assume a sufficiently fast electron transfer at this interface such that the dyes in $x = 0$ are in equilibrium with the substrate electrode at any time t (more on this in the next sections). The value of the chemical potential $E(t)$ is then correlated to the variations in the electrochemical potential applied to the system by the potentiostat. The second boundary refers to the finite thickness of the film. This constraints the gradient of the holes concentration at $x = d$. Finally, the initial condition assumes that, prior to starting the scan, all dyes are in equilibrium with the electrode at any point in the film. The use of a voltage pretreatment on the dyed TiO_2 sample at $E = E(t= 0)$ for about 10 seconds can be used to make sure that the full film is in equilibrium with the FTO electrode with $c_h(x,0) \approx 0$ given by Nernst equation if $q[E_0 - E(t = 0)]/k_BT >> 1$. Also, the effect of background light bias on the concentration of charge carriers has to be negligible.

The solution, $c_h(x,t)$, to the model S2.1 enables the determination of the diffusion current density j flowing through the sample. Considering Fick's first law for the concentration gradient, $j(t)$ can be expressed as:

$$j(t) = -qD_{app}\left.\frac{\partial c_h(0,t)}{\partial x}\right|_{x=0} \quad . \qquad \text{Eq. S2.2}$$

Finally, if the concentration of holes at $x = d$ is very low ($c_h(d,t) << c_0$) when the oxidation peak is reached, it is possible to adopt a semi-infinite slab approximation, where the diffusion problem is solved for a film of semi-infinite thickness (x ranges now from 0 to infinity). Under this assumption, from the shape of the function $j(t)$, it is possible to extract a relation between the current density peak of the cyclic voltammogram and the apparent diffusion coefficient of the species involved:[6]

$$D_{app} = 5.02 \frac{k_B T j_p^{\,2}}{q^3 c_0^{\,2} \nu} \qquad \text{Eq. S2.3}$$

The semi-infinite slab approximation is a reasonable treatment of the problem as far as the approximated diffusion length, L, calculated as $L = (D_{app}\ t_p)^{1/2}$ remains lower than the film thickness d. The term t_p can be considered as the time that the measurement takes to reach the current peak from the oxidation onset. L is an overestimate of the depth at which the holes have substantially diffused to during the time t_p. Given the thickness d of the films under investigation, this condition sets a constraint on the minimum scan rate that can be used in the experiments since, as the scan rate reduces, t_p increases. Figure S6 shows a comparison between the values of D_{app} estimated by applying the semi-infinite slab model and the actual apparent diffusion coefficients, $D_{app,real}$. $D_{app,real}$ correspond to the values used to find the solution $c_h(x,t)$ to the numerical version of the model expressed in equations S2.1 (considering a value of film thickness of d = 7 μm and for a range of scan rates). D_{app} is calculated from substituting the peak current density resulting from the numerical solution in equation S2.3. Values for the scan rates of about 0.1 to 1.5 V/s were adopted in this study, depending on the dye and the consequent value of D_{app} expected (see Figure S6). Thus, under these experimental conditions, and calculating $j_p = I_p/A$, where I_p is the measured peak current and A is the projected area of the TiO_2 film, we can extract the value of D_{app} from the cyclic voltammetry measurement using equation S2.3.

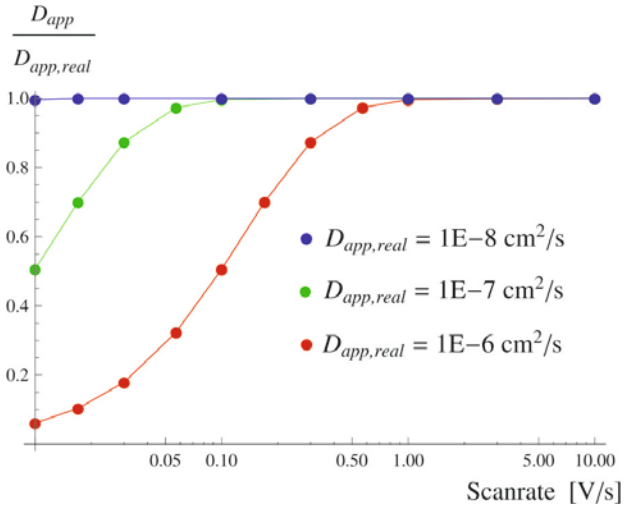

Figure S6. The ratio of estimated to actual D_{app} function of scan rate is shown for three different values of the actual apparent diffusion coefficient $D_{app,real}$. The data refer to film thickness of 7μm and to the case of no series resistance.

2.2 Validity and limitations of the method

When using the model formulated with equations S2.1, we have introduced a series of assumptions which potentially limits its validity. We consider these possible limitations below.

Influence of site occupancy and blocking on diffusion – We assume that only a single hole can reside at a molecular site on the surface lattice (although we note our evidence for the TT-1 dye that suggests a double oxidation may take place for this dye, see Figure S2). The occupancy of the sites on the surface is given by $\theta = c_h/c_0$. Thus a region of the surface in which most of the dyes are oxidized (high lattice occupancy by holes) could potentially reduce the rate of diffusion of subsequent holes in this region. We might expect this effect to result in a dependence of D_{app} on θ or c_h.

Below we show that site occupancy does *not* influence the measured value of D_{app}, so that our experimental values should be directly relatable to inter-molecular hole hopping frequency without worrying about the effects of site blocking. To demonstrate this we follow the discussion of diffusion in a Langmuir lattice described by Bisquert.[8] On a surface lattice the mean effective jump frequency of a hole, Γ, is reduced by increasing site occupancy, θ, because an attempted hopping event is only successful if the destination site is not blocked:

$$\Gamma(\theta) = (1-\theta)\Gamma(0). \qquad \text{Eq. S2.4}$$

This results in an occupancy dependent jump, or tracer, diffusion coefficient for the movement of an individual hole on the surface:

$$D_t(\theta) = (1-\theta)D_t(0). \qquad \text{Eq. S2.5}$$

However the jump diffusion coefficient, $D_t(\theta)$, does not represent the coefficient of the concentration gradient resulting in a flux of holes across the surface according to Fick's law: *hole flux* = $-D_{ch}\, \mathrm{d}c_h/\mathrm{d}x$. We will refer to this coefficient, D_{ch}, as the chemical diffusion coefficient. $D_t(\theta)$ and D_{ch} are related by a thermodynamic factor, χ_T:

$$D_{ch} = \chi_T D_t(\theta). \qquad \text{Eq. S2.6}$$

The thermodynamic factor parameterizes the effects of a statistical average of many individual hole diffusion currents in the presence of other holes. This factor can be defined in terms of the chemical potential of the holes, *E*, by:[9]

$$\chi_T = \frac{qc_h}{k_B T}\frac{\partial E}{\partial c_h} = \frac{q\theta}{k_B T}\frac{\partial E}{\partial \theta}. \qquad \text{Eq. S2.7}$$

The chemical potential for the holes on the surface lattice is given by Fermi-Dirac statistics (see equations S2.1):

$$E = E_0 + \frac{k_B T}{q}\ln\left[\theta/(1-\theta)\right], \qquad \text{Eq. S2.8}$$

so that:

$$\frac{\partial E}{\partial \theta} = \frac{k_B T}{q\theta(1-\theta)}. \qquad \text{Eq. S2.9}$$

Substituting this expression into the expression for χ_T gives:

$$\chi_T = \frac{1}{1-\theta}. \qquad \text{Eq. S2.10}$$

From equations 2.6 and 2.10 we see that this results in the chemical diffusion coefficient being independent of the lattice occupancy:

$$D_{ch} = \frac{1}{1-\theta}(1-\theta)D_t(0) = D_t(0). \qquad \text{Eq. S2.11}$$

Thus the chemical diffusion is equal to the low concentration limit of the jump diffusion coefficient, $D_t(0)$, and directly related to the jump frequency between molecules with no site

blocking, Γ(0). Experimentally we infer the apparent diffusion coefficient, D_{app}, from our CV measurements using Fick's laws since we assume the observed current is proportional to the hole concentration gradient. Thus D_{app} is directly connected to the chemical diffusion coefficient for holes on the surface as described previously (see equation 3 in main text, where D refers to D_{ch}).[7]

$$D_{app} = \alpha D_{ch} = \alpha D_t(0) = \alpha \frac{\Gamma(0) R^2}{4} \qquad \text{Eq. S2.12}$$

Accounting for series resistance - Considering the design of a typical electrochemical cell, some parasitic resistances can be identified. In Figure S7, we indicate as R_{sub} the resistance due to the FTO layer (light blue) connecting the dyed TiO_2 film (red area) to the electrical contact between sample and the potentiostat lead (V_c), and resistances due to the electrolyte between the working and reference electrodes, $R_{e,1}$, and the reference and counter electrodes, $R_{e,2}$. The relevant resistance for our analysis is $R_s = R_{sub} + R_{e,1}$ since this represents the resistance between the electrodes where the voltage is applied by the potentiostat. The capacitor $C_{d/e}$ represents the simplest model for the interface between the dyes and the electrolyte (a double channel transmission line would be more appropriate).

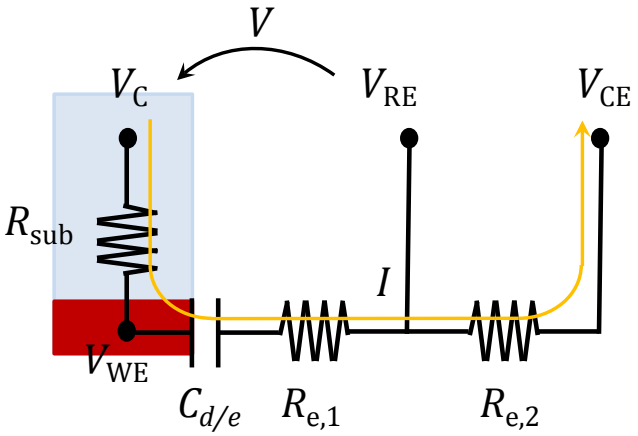

Figure S7. Equivalent circuit of the electrochemical cell used to measure CV on dye sensitized films. V is the potential applied by the potentiostat to the system and equals the difference between the potential in the sample at the position where the contact is made, V_c, and the voltage at the reference electrode V_{RE}. The effective voltage applied to the active area (in red) with respect to the electrolyte is lowered by the voltage drop on the series resistance R_{sub}.+$R_{e,1}$.

One of the signs of significant series resistance effect is the increase in the potential difference between the positive and the negative current peaks position of the CV measurement. In the case of no series resistance (and for reversible systems), this value approaches 59 mV at 25°C at any scan rate conditions, whereas it is higher than 59 mV when the voltage drop on R_s is playing a limiting role. This results in a distortion of the shape of the CV measurement due to the variation of the scan rate actually applied to the electrode. When studying the diffusion problem with the model described in Eq. S2.1, one should use the time dependent scan rate to define the chemical potential at $x = 0$. Thus the boundary condition describing $E(t)$ in equation S2.1 becomes:

$$E(t) = E(t=0) + \nu \cdot t - R_s I(t), \qquad \text{Eq. S2.13}$$

where the effective scan rate ν_{eff}, defined as the derivative of $E(t)$ with respect to t, is now a function of time. By applying this correction, it is possible to draw a better interpretation of a measured CV curve.

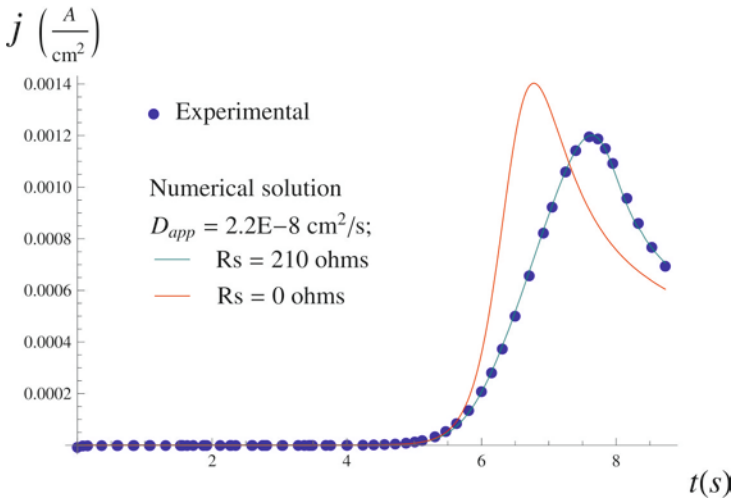

Figure S8. The experimental cyclic voltammogram performed on A2 dye sensitized TiO_2 film is compared to the calculated solution. By including the effect of series resistance it is possible to describe the shape of the current density function of time with the one dimensional diffusion model expressed in equation S2.1. The numerical solution for the same system without the effect of series resistance is also shown.

In Figure S8, the CV measurement of an A2 dye sensitized film is fitted with the model S2.1 corrected for the effects of series resistance according to equation S2.13. The calculation of D_{app} from the current peak of the experimental data with equation S2.3 would give in this case 1.6 10^{-8} cm^2/s, whereas the fit returns 2.2 10^{-8} cm^2/s. Figure S8 also shows what the CV curve would look like if there were no series resistance limitations (i.e. with $R_s = 0$ and $D_{app} =$ 2.2 10^{-8} cm^2/s). In this case equation S2.3 returns the same value of D_{app} that was set for the simulation.

Despite the good quality of the fit in the example of Figure S8, almost all the CV curves that we measured showed a broader peak than the numerical solution. A full series resistance compensation was therefore not possible with the oversimplified model described so far. Kinetic limitations at the interface (discussed below) and energetic disorder are thought to be the main factors determining the broadening of the CV peak.

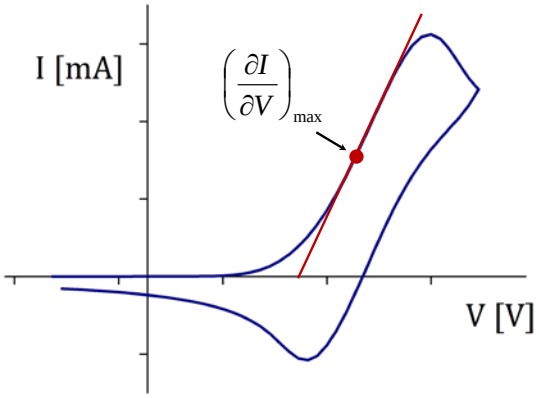

Figure S9. The maximum derivative value in the oxidation peak of the I-V curve measured via cyclic voltammetry can be used to estimate the maximum variation of the effective scan rate with respect to the set value.

Given this limitation, we introduce a quick method to estimate the variation in effective scan rate in a CV measurement and a way to extract the range of possible values of D_{app}. The peak value of the fractional change of the effective scan rate in the positive scan is proportional to the series resistance R_s and to the maximum derivative of the current with respect to the voltage in the oxidation curve (see Figure S9).

$$\frac{\nu_{eff,\min} - \nu}{\nu} = -\left.\frac{\partial I}{\partial V}\right|_{\max} R_s \qquad \text{Eq. S2.14}$$

In cases where the series resistance of the system is negligible, v_{eff} equals the value of the applied scan rate (v) set during the measurement. Conversely, substituting $v_{eff,min}$, calculated with Eq. S2.14, into Eq. S2.3 enables the upper limit of the holes apparent diffusion coefficient to be estimated. In the example illustrated in Figure S8, using the minimum scan rate calculated with this simple model to extract D_{app} using equation S2.3 would give 2.9 10^{-8} cm^2/s considering a series resistance of 210 Ω (see fit in Figure S8), compared to the actual value of 2.2 10^{-8} cm^2/s returned by the fit.

However, the value of the series resistance might not be easy to measure. Again one can find a slight overestimation of it by considering the ratio between the differences in voltage and current ΔV and ΔI corresponding to the oxidation and reduction peaks (in the case of Figure S8 this estimate would be 285 Ω and would lead to a D_{app} of 4 10^{-8} cm^2/s). This approach ignores any shift in the peaks' positions, even in absence of series resistance, related to the diffusion process, to the kinetic limitations (see below) and the reversibility of the system. Instead of using ΔV for the calculation of R_s, one can use ΔV - η, where η would take into account the overpotential at the FTO/dyed-TiO_2 interface and the nominal peaks shift. One way to estimate η is to perform CV measurements on samples of the same material with different areas or on a single sample with slightly different scan rate (in order not to change the kinetics) and then take the intercept of ΔV plotted against ΔI. The analysis of the data reported in the main text with this method shows values for the overestimated D_{app} which are typically higher by a factor between 1.5 and 4. The corresponding activation energies extracted from the plot of these values still match the ones reported within experimental error, apart from the case of D149 where, considering a value of η = 0.23V, the corresponding activation energy is 275 ± 27 meV against the 244 ± 22 meV reported in the main text. Although the values are still close within 2σ, considering that η is in fact variable with temperature, one can expect an even higher discrepancy.

Series resistance effects can be reduced by reducing the overall current flowing in the cell. This can be achieved by reducing the area of the TiO_2 films (in this work, the dyed TiO_2

films we used were between 20 and 40 mm^2 in area) and by using as low as possible values of scan rate, which on the other hand have to comply with the semi-infinite slab approximation previously described.

Kinetic limitations at the FTO dye interface - The definition of the concentration of holes at $x = 0$ relies on the validity of the boundary condition defined by Nernst equation:

$$E = E_0 + \frac{k_B T}{nq} \ln \frac{c_{ox}}{c_{red}} \qquad \text{Eq. S2.15}$$

where the ratio between the concentrations of oxidized and reduced species (c_{ox} and c_{red}) is shown to be related to the relative value of the chemical potential at the working electrode E with respect to the formal redox potential E_0 of the reaction. Here n is the number of electrons involved in the reaction (in this case n=1). This relation is valid as long as the electrode is in equilibrium with the redox species at the interface, namely the electron transfer between the FTO substrate and the dye molecules in its proximity has to be sufficiently rapid. When this assumption is not met by the system conditions, the kinetics of charge transfer should be taken into account. The effect of kinetic limitations is similar to the one previously discussed for the series resistance, that is a shift of the current peaks positions in opposite direction.[6] This can be modelled by introducing an overpotential which further reduces the effective scan rate and leads to further underestimation of D_{app}. However, if we consider the Butler-Volmer equation, we would expect a non-linear relation between overpotential and current density.[10] This implies that estimating the variation of v_{eff} due to charge transfer kinetic limitations at the interface with equation S2.13 would require the use of a current density dependent value of R_s. A final remark is that kinetic limitations depend on the current density exchanged at the FTO/dyed TiO_2 interface. For this reason, while a reduction in scan rate is still beneficial for decreasing their contribution, reducing the area of the TiO_2 film does not have any effect.

Ambipolar diffusion - The diffusion phenomenon observed in the system we investigated and described by equations S2.1 is an ambipolar diffusion process, since charges in the electrolyte must be rearranged to maintain local charge neutrality as holes diffuse across the TiO_2 surface. For this reason, equation S2.3 is only valid under the assumption that the

transport of the holes is a more limiting factor than the transport of ions in the surrounding electrolyte. The diffusion coefficient used in equation S2.3 refers in general to an ambipolar diffusion coefficient D_{amb}, which is related to the holes apparent diffusion coefficient D_{app} through the following equation:

$$D_{amb} = \frac{c_h + c_i}{\frac{c_h}{D_i} + \frac{c_i}{D_{app}}} \qquad \text{Eq. S2.16}$$

According to this relation, the value of the diffusion coefficient measured in cyclic voltammetry D_{amb} is between the values D_{app} and the diffusion coefficient of the ions in solution (D_i). In particular, D_{amb} varies depending on the concentration of the ions c_i, given a certain hole concentration c_h. We may expect a slightly different formulation of D_{amb} when considering the different dimensionalities of the monolayer and the electrolyte.

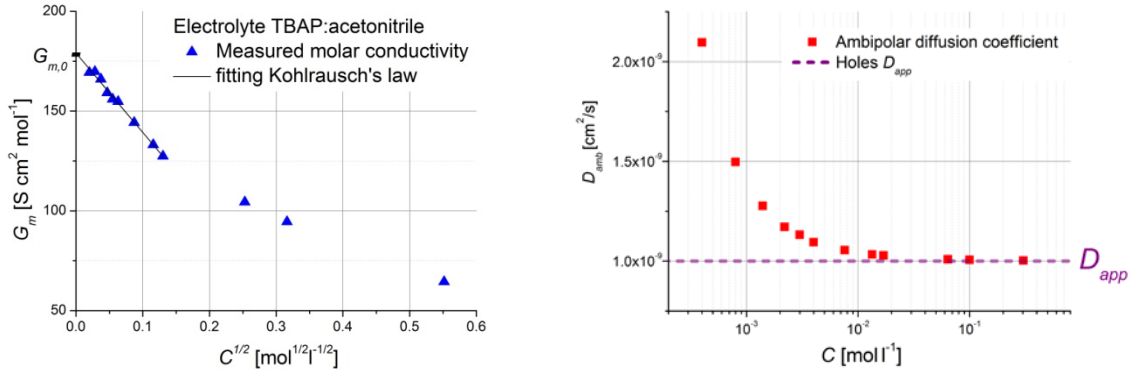

Figure S10. Molar conductivity of TBAP in acetonitrile (left) and estimated ambipolar diffusion coefficient (right) as a function of electrolyte concentration. When sufficiently high concentration values are used, D_{amb} shows a plateau at the value of D_{app} (in the right graph D_{app} =10^{-9} cm^2/s and c_h = 10^{20} cm^{-3}).

We performed measurements of the molar conductivity of the electrolyte composition used in this study to calculate D_i. Nevertheless, this quantity varies as a function ionic concentration. A correct characterization of the parameters c_i and D_i goes beyond the scope of our study. Here, we want to suggest a method to analyze this problem on a first order approximation. We assume that the system can be described by considering two extreme situations.

If the electrolyte conductivity is described by a "viscosity model" then D_i depends on the electrolyte viscosity, which increases with ionic concentration c_i, and all ions are assumed active. The measured conductivity of the electrolyte, G, can be then related to the diffusion coefficient D_i, by:

$$G = \frac{q^2 c_i D_i}{k_B T} \quad . \qquad \text{Eq. S2.17}$$

where in this case, c_i is the concentration of all ions in solution.

Alternatively, using an "ion pairing" model, we can consider the ions diffusing with D_i equal to D_0, which is the diffusion coefficient at infinite dilution conditions. To explain the drop in molar conductivity, the effective concentration of active ions must be less than the total ionic concentration. In this model, fitting molar conductivity (G_m) data measured at low ionic concentrations with Kohlrausch's law (Eq. S2.18) enables the extraction of the molar conductivity at infinite dilution condition $G_{m,0}$: [11]

$$G_m = G_{m,0} - \kappa c_i^{0.5}. \qquad \text{Eq. S2.18}$$

From the value of $G_{m,0}$, which is indicated as the intercept of the linear fit in Figure S10 in the left graph, we can calculate the diffusion coefficient of the ions at infinite dilution condition as $D_0 = G_{m,0}\, k_B T/q^2$. The effective concentration of active ions c_i at a certain concentration is then calculated by rearranging equation S2.17, given the measured conductivity of the electrolyte G and considering $D_i = D_0$.

Since acetonitrile gives rise to strong electrolyte solutions, the two models give very similar results. However, the "ion pairing" model gives an overestimate of the difference between D_{amb} and D_{app}. For this reason it is good to adopt it to keep a more conservative approach, especially in case of less polar solvent which may show significant difference between the two estimates. The use of 0.1 M as reference concentration results in accurate determination of D_{app}. In Figure S10, the measurement of the molar conductivity of TBAP in acetonitrile at 22°C and a reference value of 10^{-9} cm^2/s for D_{app} are considered. Given a maximum acceptable error for the determination of D_{app} from the measurement of D_{amb}, a constraint on the minimum molarity of the electrolyte is thus set through these considerations.

Supplementary references

1. A. Fattori, L. M. Peter, H. Wang, H. Miura, and F. Marken, *J. Phys. Chem. C*, 2010, **205**, 11822–11828.

2. N. R. Neale, N. Kopidakis, J. van de Lagemaat, M. Grätzel, and A. J. Frank, *J. Phys. Chem. B*, 2005, **109**, 23183–9.

3. A. Fattori, L. M. Peter, S. R. Belding, R. G. Compton, and F. Marken, *J. Electroanal. Chem.*, 2010, **640**, 61–67.

4. A. Fattori, L. M. Peter, K. L. McCall, N. Robertson, and F. Marken, *J. Solid State Electrochem.*, 2010, **14**, 1929–1936.

5. URL: http://www.consultrsr.com/resources/ref/refpotls.htm

6. A. J. Bard and L. R. Faulkner, *Electrochemical Methods*, Second Edi., 2001.

7. V. Vaissier, P. R. F. Barnes, J. Kirkpatrick, and J. Nelson, *Phys. Chem. Chem. Phys.*, 2013, **15**, 4804–14.

8. J. Bisquert, *J. Phys. Chem. B*, 2004, **108**, 2323–2332.

9. R. Gomer, *Reports Prog. Phys.*, 1990, **53**, 917–1002.

10. A. J. Bard and L. R. Faulkner, *Electrochemical methods*, 2001.

11. P. Atkins and J. de Paula, *Physical Chemistry*, 2006.